International Journal for Parasitology: Drugs and Drug Resistance 17 (2021) 67–79

Contents lists available at ScienceDirect

International Journal for Parasitology: Drugs and Drug Resistance

journal homepage: www.elsevier.com/locate/ijpddr

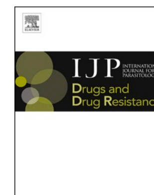

Antiamoeboid activity of squamins C–F, cyclooctapeptides from *Annona globifora*

Rubén L. Rodríguez-Expósito [a,b,c], Javier Sosa-Rueda [f], María Reyes-Batlle [a,b,c], Ines Sifaoui [a,b,c], Francisco Cen-Pacheco [d,f,**], Antonio Hernández Daranas [g], Ana R. Díaz-Marrero [d], José E. Piñero [a,b,c,***], José J. Fernández [d,e,****], Jacob Lorenzo-Morales [a,b,c,*]

[a] *Instituto Universitario de Enfermedades Tropicales y Salud Pública de Canarias (IUETSPC), Universidad de La Laguna (ULL), Avda. Astrofísico Francisco Sánchez s/n, 38203, La Laguna, Tenerife, Spain*
[b] *Departamento de Obstetricia, Ginecología, Pediatría, Medicina Preventiva y Salud Pública, Toxicología, Medicina Legal y Forense y Parasitología, Universidad de La Laguna, 38203, La Laguna, Tenerife, Spain*
[c] *Red de Investigación Cooperativa en Enfermedades Tropicales (RICET), Madrid, Spain*
[d] *Instituto Universitario de Bio-Orgánica Antonio González (IUBO AG), Universidad de La Laguna (ULL), Avda. Astrofísico Francisco Sánchez 2, 38206, La Laguna, Tenerife, Spain*
[e] *Departamento de Química Orgánica, Universidad de La Laguna (ULL), Avda. Astrofísico Francisco Sánchez s/n, 38206, La Laguna, Tenerife, Spain*
[f] *Facultad de Bioanálisis, Universidad Veracruzana (UV), Agustín de Iturbide s/n, Centro, 91700Veracruz, Veracruz, Mexico*
[g] *Instituto de Productos Naturales y Agrobiología (IPNA), Consejo Superior de Investigaciones Científicas (CSIC), Avda. Astrofísico Francisco Sánchez 3, 38206, La Laguna, Tenerife, Spain*

ARTICLE INFO

Keywords:
Squamin
Cyclopeptide
Acanthamoeba
Annona
Antiamoeboid

ABSTRACT

Free-living amoebae of *Acanthamoeba* spp. are causative agents of human infections such as granulomatous amoebic encephalitis (GAE) and *Acanthamoeba* keratitis (AK). The exploration of innovative chemical entities from natural sources that induce intrinsic apoptotic pathway or a Programmed Cell Death (PCD) in *Acanthamoeba* protozoa is essential to develop new therapeutic strategies. In this work, the antiamoeboid activity of squamins C–F (**1**–**4**), four cyclooctapeptides isolated from *Annona globiflora* was tested *in vitro* against *Acanthamoeba castellanii* Neff, *A. polyphaga*, *A. quina*, and *A. griffini*, and a structure–activity relationship was also established. The most sensitive strain against all tested cyclooctapeptides was *A. castellanii* Neff being the R conformers of the S-oxo-methionine residue, squamins D (**2**) and F (**4**), the most active against the trophozoite stage. It is remarkable that all four peptides showed no cytotoxic effects against murine macrophages cell line J774A.1. The analysis of the mode of action of squamins C–F against *A. castellanii* indicate that these cyclopeptides induced the mechanisms of programmed cell death (PCD). All peptides trigger mitochondrial damages, significant inhibition of ATP production compared to the negative control, chromatin condensation and slight damages in membrane that affects its permeability despite it conserves integrity at the IC_{90} for 24 h. An increase in reactive oxygen species (ROS) was observed in all cases.

* Corresponding author. Instituto Universitario de Enfermedades Tropicales y Salud Pública de Canarias (IUETSPC), Universidad de La Laguna (ULL), Avda. Astrofísico Francisco Sánchez s/n, 38203, La Laguna, Tenerife, Spain.
** Corresponding author. Instituto Universitario de Bio-Orgánica Antonio González (IUBO AG), Universidad de La Laguna (ULL), Avda. Astrofísico Francisco Sánchez 2, 38206, La Laguna, Tenerife, Spain.
*** Corresponding author. Instituto Universitario de Enfermedades Tropicales y Salud Pública de Canarias (IUETSPC), Universidad de La Laguna (ULL), Avda. Astrofísico Francisco Sánchez s/n, 38203, La Laguna, Tenerife, Spain.
**** Corresponding author. Instituto Universitario de Bio-Orgánica Antonio González (IUBO AG), Universidad de La Laguna (ULL), Avda. Astrofísico Francisco Sánchez 2, 38206, La Laguna, Tenerife, Spain.
E-mail addresses: fcen@uv.mx (F. Cen-Pacheco), jpinero@ull.edu.es (J.E. Piñero), jjfercas@ull.edu.es (J.J. Fernández), jmlorenz@ull.edu.es (J. Lorenzo-Morales).

https://doi.org/10.1016/j.ijpddr.2021.08.003
Received 13 July 2021; Received in revised form 3 August 2021; Accepted 9 August 2021
Available online 11 August 2021
2211-3207/© 2021 The Authors. Published by Elsevier Ltd on behalf of Australian Society for Parasitology. This is an open access article under the CC BY-NC-ND license (http://creativecommons.org/licenses/by-nc-nd/4.0/).

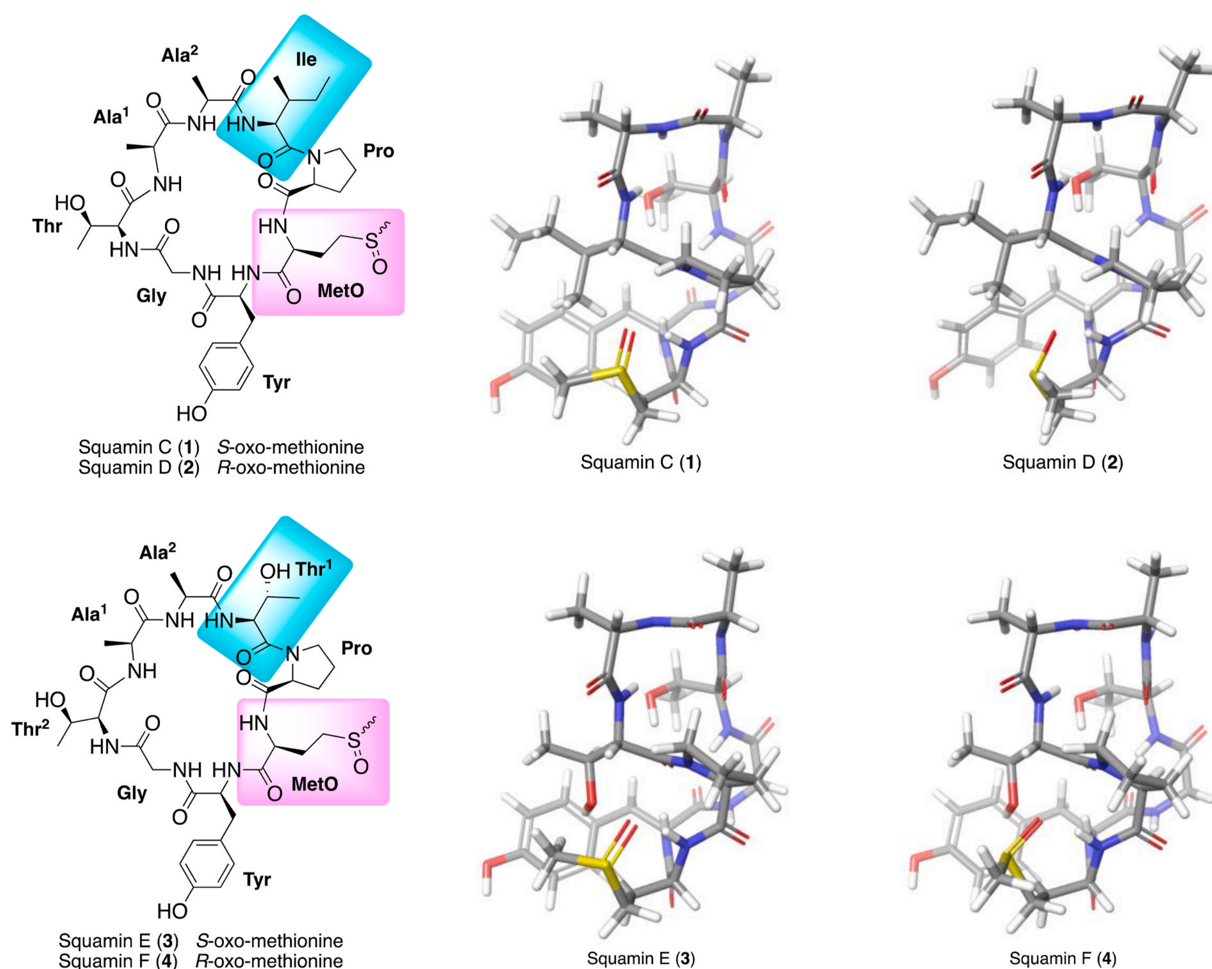

Fig. 1. Chemical structure and 3D minimal conformation of squamins C–F (**1**–**4**).

Table 1
Antiamoebic activity of squamins C–F (**1**–**4**) against trophozoites of *Acanthamoeba* spp. strains and cytotoxicity against murine macrophages cell line J774A.1 (ATCC TIB-67).

Compounds	*A. castellanii* Neff IC_{50} (μM)	*A. polyphaga* IC_{50} (μM)	*A. griffini* IC_{50} (μM)	*A. quina* IC_{50} (μM)	J774A.1 CC_{50} (μM)
Squamin C (**1**)	20.77 ± 3.48	71.78 ± 0.41	38.81 ± 7.34	24.28 ± 0.64	>200
Squamin D (**2**)	18.38 ± 1.14	71.57 ± 0.14	39.53 ± 5.90	26.52 ± 0.87	>200
Squamin E (**3**)	21.00 ± 0.86	62.19 ± 15.52	44.75 ± 2.06	25.82 ± 0.99	>200
Squamin F (**4**)	18.02 ± 3.28	64.08 ± 12.42	50.49 ± 6.92	30.32 ± 0.27	>200
Clorhexidine	5.97 ± 1.76	9.41 ± 0.16	7.38 ± 1.94	4.04 ± 0.48	14.64 ± 0.77
Voriconazole	2.69 ± 0.83	28.91 ± 6.32	0.29 ± 0.06	1.32 ± 0.08	21.64 ± 2.20

Table 2
Antiamoebic activity of squamins C–F (**1**–**4**) against the cyst stage of *Acanthamoeba* spp. strains.

Compounds	*A. castellanii* Neff IC_{50} (μM)	*A. polyphaga* IC_{50} (μM)	*A. griffini* IC_{50} (μM)	*A. quina* IC_{50} (μM)
Squamin C (**1**)	73.07 ± 4.10	73.30 ± 0.38	>100	>100
Squamin D (**2**)	39.02 ± 6.61	72.94 ± 0.53	>100	>100
Squamin E (**3**)	44.53 ± 0.33	73.62 ± 0.09	>100	>100
Squamin F (**4**)	52.40 ± 6.89	73.63 ± 0.17	>100	>100
Clorhexidine	14.64 ± 0.77	5.59 ± 0.004	5.60 ± 0.07	5.31 ± 0.48
Voriconazole	21.64 ± 2.20	55.33 ± 1.82	37.61 ± 4.39	24.06 ± 0.85

1. Introduction

Acanthamoeba spp. are ubiquitous free-living amoebae known as causative agent in human of granulomatous amoebic encephalitis (GAE), a chronic progressive disease of the central nervous system often fatal in patients, and *Acanthamoeba* keratitis (AK), a painful corneal infection in immunocompetent individuals, mostly related to contact lenses wearers (Lorenzo-Morales et al., 2015; Rodríguez-Martín et al., 2018). The life cycle of *Acanthamoeba* involves both an active vegetatively growing trophozoite stage and a double-walled dormant cyst stage, which is highly resistant form to disinfectant and the current medical therapy management (Siddiqui and Khan, 2012; Kot et al., 2018). Therefore, due to the difficulty to eradicate *Acanthamoeba* from the infection site and the frequent development of undesirable side effects in treated patients, further research is needed to exploit new amoebicidal agents and therapeutic strategies.

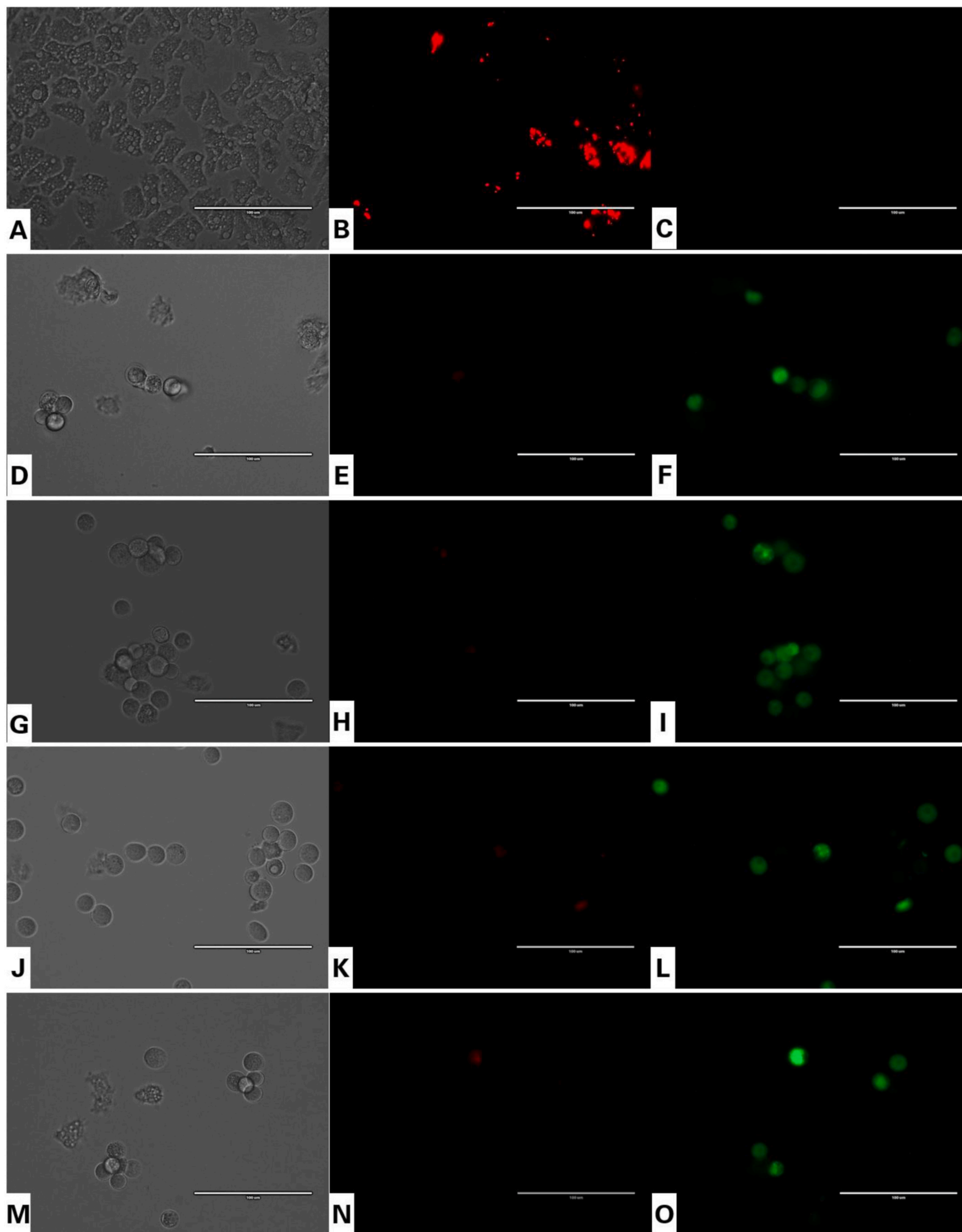

Fig. 2. Effect of IC_{90} of squamin C (D, E, F), squamin D (G, H, I), squamin E (J, K, L) and squamin F (M, N, O) on the mitochondrial potential of *Acanthamoeba castellanii* Neff trophozoites, where JC-1 dye remained in the cytoplasm in its monomeric form, green fluorescence, due to the collapse of the mitochondrial potential (C, F, I, L, O). Compared with the control (A to C), JC-1 dye accumulates in the mitochondria of healthy trophozoites as aggregates (red fluorescence) in untreated amoebae. All images (40x) are based on Live Cell Imaging Microscope EVOS FL Cell Imaging System (Scale Bar 100 µm). (For interpretation of the references to colour in this figure legend, the reader is referred to the Web version of this article.)

New natural products such as metabolites isolated from roots, seeds, leaves, fruits or stem bark of plants have been identified by their high antiparasitic efficacy and selectivity (Wink, 2012; Ohashi et al., 2018; Chegeni et al., 2020). Notwithstanding, the exploration of innovative chemical entities that develop intrinsic apoptotic pathway or induce a Programmed Cell Death (PCD) in the protozoa *Acanthamoeba* is essential to avoid the inflammation damages caused by the host immune system in response to amoeba infection (Baig et al., 2017).

Despite the significant number of ethnopharmacological records from different cultures, there are few reports on the use of the genus *Annona* to treat parasitic diseases. To the best of our knowledge, these studies have focused on protozoal diseases, such as leishmaniasis, trypanosomiasis and malaria (Quílez et al., 2018). Nonetheless, metabolites isolated from the *Annona* genus stand out for their potent cytotoxic, antibacterial, antioxidant, vasorelaxant or anti-inflammatory activities, being few the reports referred to the antiprotozoal properties (Quílez et al., 2018; Leite et al., 2020). Among compounds produced by *Annona* species, cyclic peptides comprise an interesting class of molecules that show a great variety in the number and composition of aminoacid residues. Some of them have been submitted to clinical trials, due to their attractive pharmacological properties (Dahiya and Dahiya, 2021; Tan and Zhou, 2006; Wang et al., 2017). On the other hand, many cyclopeptides have been used as research tools in molecular and biological processes involved in cellular regulation (Sarabia et al., 2004).

There are around 20 species of *Annona* genus, distributed mainly in tropical regions of the Southeast of Mexico (Anaya-Esparza et al., 2020). *Annona globiflora* Schltdl. (Annonaceae) is an endemic species, named “chirimoyito” by native people, which grows in the wild central area of the state of Veracruz (Escobedo-López et al., 2019). In a previous work, we have reported the isolation of four cyclopeptides named squamins C–F (**1**–**4**) of the seeds of *A. globiflora*, their structures were determined using NMR spectroscopy techniques, ESI-HRMS data and Marfey’s method (Sosa-Rueda et al., 2021). In this work, squamins C–F (**1**–**4**), were evaluated *in vitro* against *Acanthamoeba castellanii* Neff, *A. polyphaga*, *A. quina*, and *A. griffini*, and a structure–activity relationship was also established.

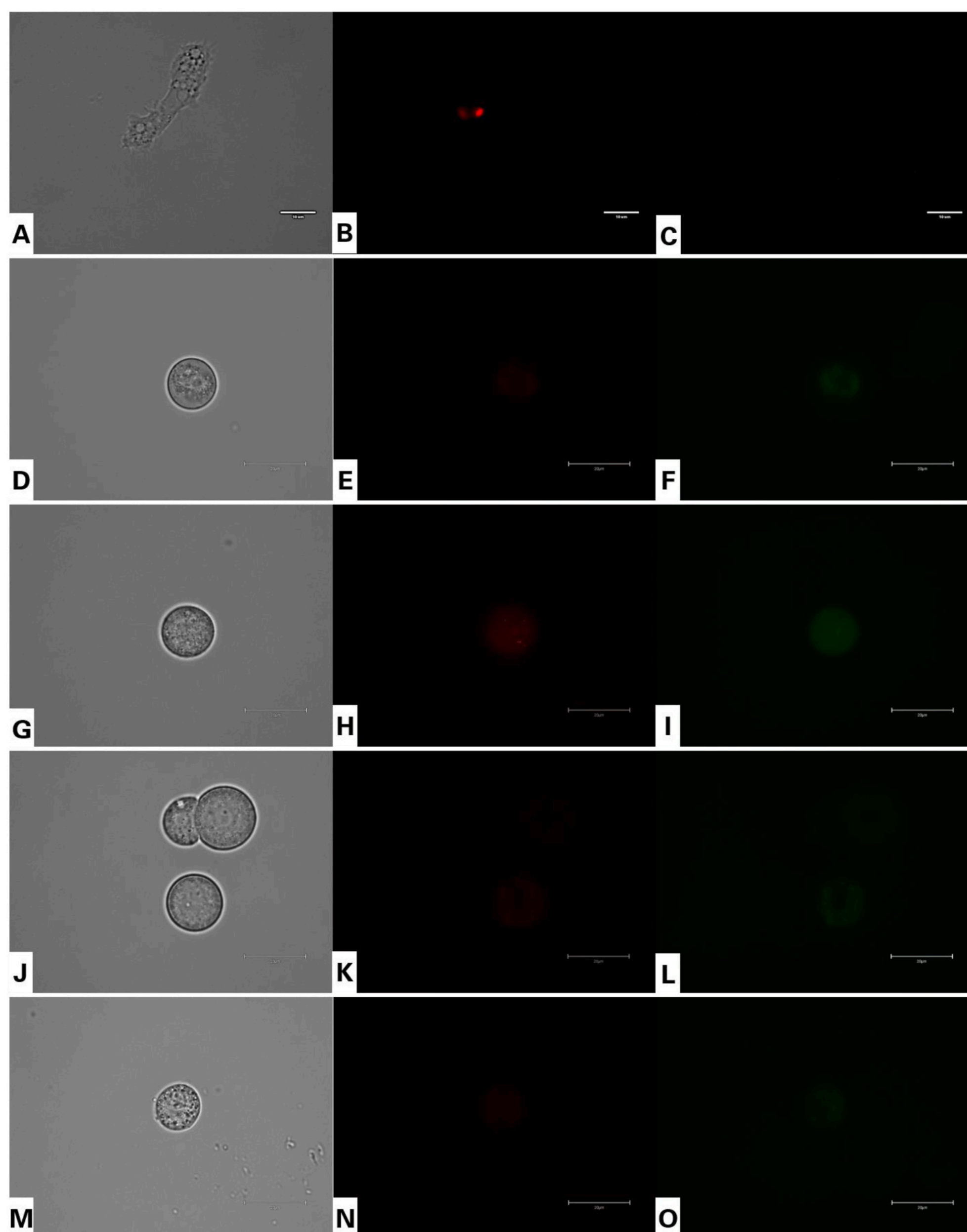

Fig. 3. Images at 100x magnification of the effect of IC_{90} of peptide C (D, E, F), peptide D (G, H, I), peptide E (J, K, L) and peptide F (M, N, O) on the mitochondrial potential of *Acanthamoeba castellanii* Neff trophozoites. All images are based on Live Cell Imaging Microscope EVOS FL Cell Imaging System (Scale Bar 10 and 20 μm).

2. Materials and methods

2.1. General methods

. All solvents were dried and distilled under argon immediately prior to use or stored appropriately. Melting points were determined on a Büchi B-540 model. Optical rotations were determined on a PerkinElmer 343 polarimeter (Waltham, MA, USA) using a sodium lamp operating at 589 nm. NMR spectra were performed on Bruker Avance 500, or 600 instruments (Bruker Biospin, Falländen, Switzerland) at 300 K, and coupling constants are given in Hz. COSY, 1D/2D TOCSY, HSQC, HMBC data were processed using Topspin or MestReNova software (Mestrelab Research, S.L., Santiago de Compostela, Spain). Mass spectra were recorded on an LCT Premier XE Micromass spectrometer using electrospray ionization. EnSpire® Multimode Reader (Perkin Elmer, Waltham, MA, USA) used absorbance values of alamarBlue® reagent (Bio-Rad Laboratories, Oxford, UK). Thin Layer Chromatography (TLC) was performed in Al Si gel. TLC plates were visualized by UV light (254 nm) and by adding a phosphomolybdic acid solution 10% (*w/v*) in EtOH.

2.2. Plant material

The seeds of *Annona globiflora* Schltdl. (Annonaceae) were collected from the municipality Medellin de Bravo, Veracruz Ignacio de la Llave (México) in May 2018 (wet season) (19°01′44.5″N 96°08′20.4″W) and identified by taxonomists of the Institute for Biological Research at Veracruz University, Xalapa, Mexico.

2.3. Isolation of Annona metabolites

Seeds of *Annona globiflora* (500 g) were dried in the dark and triturated (particle size 0.1–0.5 cm). The resulting particles were extracted using MeOH (4 × (3 L × 3 h)) at room temperature. Next, the extract was concentrated *in vacuo* to yield a brownish viscous extract of 12.5 g. This

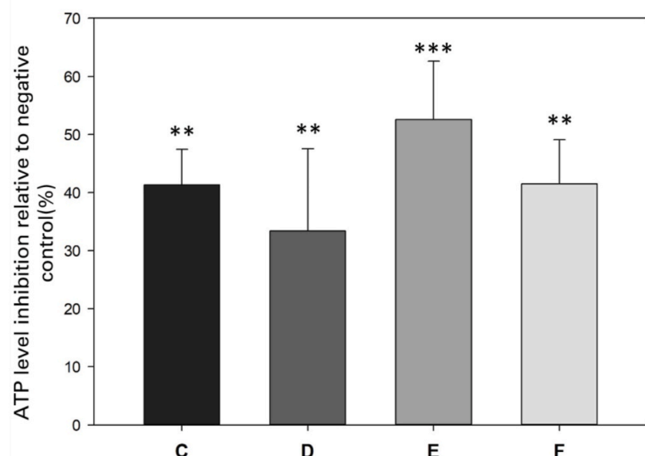

Fig. 4. Inhibition in the ATP level produced by the peptides C, D, E and F IC_{90} values against *Acanthamoeba castellanii* Neff using CellTiter-Glo® luminescent cell viability assay related to the negative control. (***$p < 0.001$; **$p < 0.01$).

material was fractionated by liquid-liquid extraction, using the modified Kupchan method (Kupchan et al., 1973; Cen-Pacheco et al., 2019). The enriched peptide fraction (AcOEt; 416 mg) was chromatographed using medium pressure liquid chromatography Lobar LiChroprep-RP19 (Merck, Darmstadt, Germany) with MeOH/H_2O (7:3), then finally purified in a μ-Bondapack C-18 HPLC column (Waters, Wexford, Ireland) using MeOH:H_2O as mobile phase. This procedure yielded 2.9 mg of squamin C (**1**), 2.5 mg of D (**2**), 1.9 mg of E (**3**) and 1.5 mg of F (**4**).

2.4. *Acanthamoeba strains*

The anti-*Acanthamoeba* activity of squamins C–F (**1**–**4**) was evaluated against the type strains *Acanthamoeba castellanii* Neff, genotype T4 (ATCC 30010) *Acanthamoeba polyphaga*, genotype T4 (ATCC 30461) and *Acanthamoeba quina*, genotype T4 (ATCC 50241), and the *Acanthamoeba griffini*, genotype T3 obtained in a previous study (González-Robles et al., 2014). Those strains were grown axenically in Peptone Yeast Glucose (PYG) medium (0.75% (w/v) proteose peptone, 0.75% (w/v) yeast extract, and 1.5% (w/v) glucose) containing 40 μg/ml of gentamicin (Biochrom AG, Cultek, Granollers, Barcelona, Spain).

2.5. *In vitro effect against the trophozoite stage of Acanthamoeba spp*

The effect of the squamins C–F (**1**–**4**) against the trophozoite stage of *Acanthamoeba* strains was determined *in vitro* using the alamarBlue® method previously described (Martín-Navarro et al., 2008). *Acanthamoeba* spp. trophozoites were culture on a 96-well microtiter plates (50 μL from a stock solution of $5{\cdot}10^4$ cells/mL). After trophozoites attachment, 50 μL of serial dilutions of each molecule were added to each well. Finally, alamarBlue® Reagent (Life Technologies, Madrid, Spain) was placed into each well at an amount equal to 10% of the final volume and the plates were incubated during 96 h at 26 °C with a soft agitation. The plates were analysed using an EnSpire® Multimode Plate Reader (Perkin Elmer, Madrid, Spain) using a test wavelength of 570 nm and a reference wavelength of 630 nm.

2.6. *In vitro effect against of Acanthamoeba spp. cysts*

The cysticidal activity was evaluated by the alamarBlue® assay at 168 h and confirmed visually by inverted microscopy (Leica DMIL, Barcelona, Spain). Cysts of the *Acanthamoeba* strains were prepared as it has been described before (Martín-Navarro et al., 2015) and following the instructions of the defined protocol (Sifaoui et al., 2018) with some modifications. 50 μL of $5{\cdot}10^4$ cysts/mL as final concentration of mature cysts of *Acanthamoeba* strains were cultivated in PYG medium in triplicate on a 96-well plate with 50 μL of serial dilutions of squamins C–F (**1**–**4**). *Acanthamoeba* spp. cysts incubated in PYG medium were used as negative control. After an incubation of 168 h at 26 °C, the plate was centrifuged at 3000 rpm for 10 min and the supernatant was removed. A total of 100 μL of fresh PYG medium were added to each assay well and the alamarBlue® Reagent was placed into each well at 10% and the plates were incubated 168 h at 26 °C. The plates were analysed using an EnSpire® Multimode Plate Reader as it was described above.

2.7. *Cytotoxicity assays*

In order to evaluate the toxicity of the evaluated molecules, the murine macrophage cell line J774A.1 (ATCC TIB-67) was used. Macrophages were cultured in RPMI (Roswell Park Memorial Institute, 1640 medium) supplemented with 10% fetal bovine serum at 37 °C and 5% CO_2 atmosphere. The cytotoxic effect of the evaluated molecules was tested using the alamarBlue® method as described in previous studies (Rodríguez-Expósito et al., 2021).

2.8. *Analysis of mitochondrial membrane potential*

The collapse of an electrochemical gradient across the mitochondrial membrane during apoptosis was detected with the JC-1 mitochondrial membrane potential detection kit (Cayman Chemicals, Vitro SA, Madrid, Spain). Trophozoites were cultured on 96-well plate at a final concentration of 10^5 cells/mL with PYG medium, treated with IC_{90} of the tested compounds for 24 h and incubated with JC-1 reagent following the manufacturer's instructions. Images were taken on EVOS FL Cell Imaging System AMF4300, Life Technologies, Madrid, Spain. The staining pattern allows the identification of two groups in a cellular population: live cells will show only red fluorescence; and cells with low mitochondrial potential, undergoing programmed cell dead (PCD), will show a higher level of green and red fluorescence.

2.9. *Measurement of ATP*

The ATP level was measured using a CellTiter-Glo Luminescent Cell Viability Assay (PROMEGA BIOTECH IBÉRICA S.L, Madrid, Spain). The effect of squamins C–F (**1**–**4**) on the ATP production was evaluated by incubating 10^5 of cells/mL in PYG medium with the previously calculated IC_{90} for 24 h at 26 °C.

2.10. *Double-stain assay for programmed cell death determination*

A double-stain apoptosis detection kit (Hoechst 33342/PI) (Life Technologies, Madrid, Spain) and an EVOS FL Cell Imaging System AMF4300, (Life Technologies, Madrid, Spain) were used in this assay. The experiment was carried out by following the manufacturer's recommendations, and 10^5 cells/mL well were incubated for 24 h with the previously calculated IC_{90} of squamins C–F (**1**–**4**). As previously reported (Sifaoui et al., 2020), the double-staining pattern allows the identification of three groups in a cellular population: live cells will show only a low level of blue fluorescence, cells undergoing PCD will show a higher level of blue fluorescence (as chromatin condenses), and dead cells will show low-blue and high-red fluorescence (as the Propidium Iodide stain (Life Technologies, Madrid, Spain) enters the nucleus).

2.11. *Plasma membrane permeability*

The SYTOX Green assay (Life Technologies, Madrid, Spain) was performed to detect alterations on plasmatic membrane permeability in treated amoebae. First, 10^5 trophozoites were incubated with the previously calculated IC_{90} of each evaluated molecule. After 24 h of

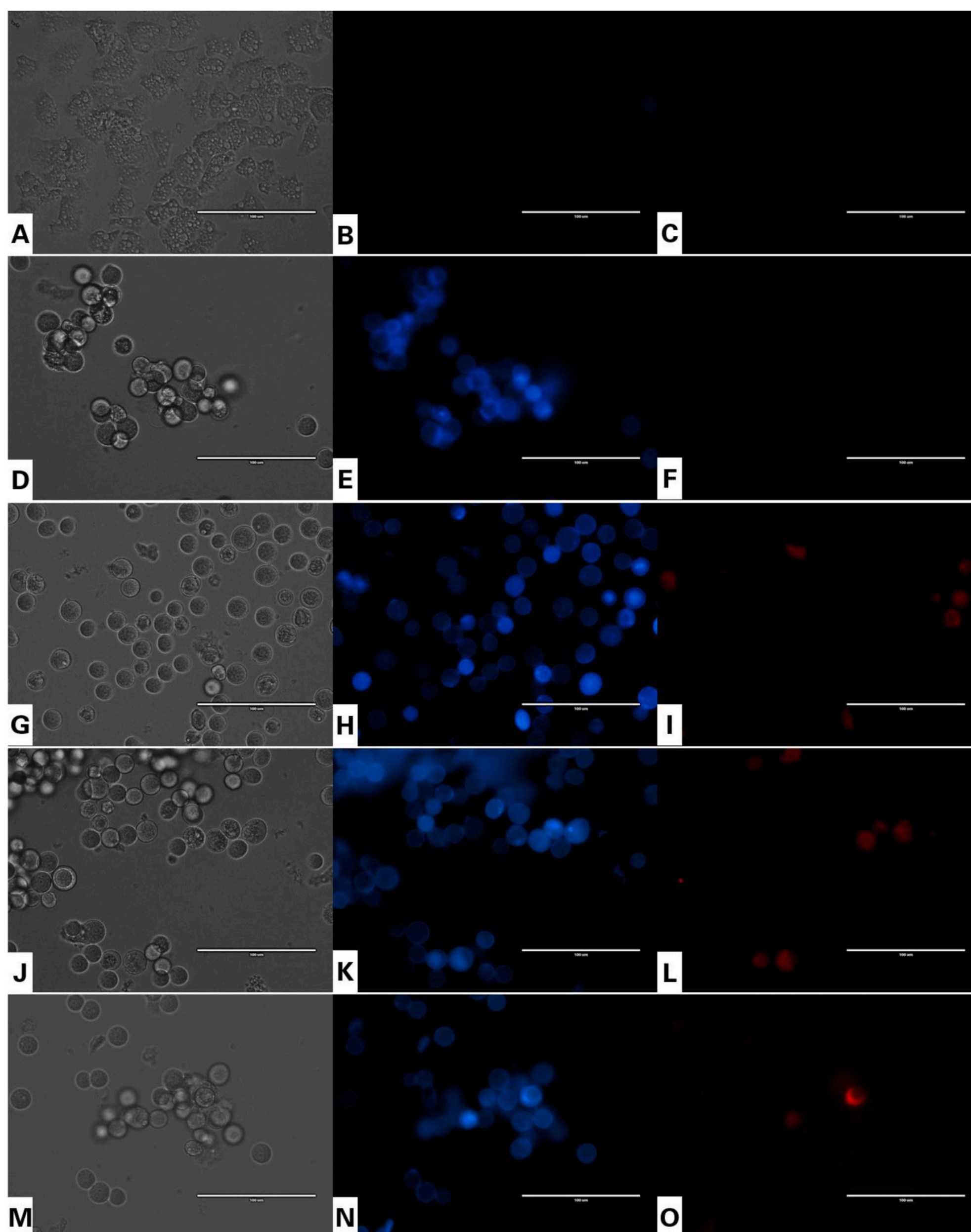

Fig. 5. *Acanthamoeba castellanii* Neff trophozoites incubated with IC_{90} of squamin C (D, E, F), squamin D (G, H, I), squamin E (J, K, L) and squamin F (M, N, O) for 24 h. Negative control (A, B, C). Hoechst stains treated trophozoites nuclei in bright blue, showing chromatin condensation, and red fluorescence corresponds to the propidium iodide dye, which stains the nuclei of death cells. All images (40x) are based on Live Cell Imaging Microscope EVOS FL Cell Imaging System (Scale Bar 100 μm). (For interpretation of the references to colour in this figure legend, the reader is referred to the Web version of this article.)

incubation, the SYTOX Green was added at a final concentration of 1 μM. The images were taken after 15 min of incubation in darkness with EVOS FL Cell Imaging System AMF4300 (Life Technologies, Madrid, Spain).

2.12. Intracellular ROS production using CellROX® Deep Red staining

The generation of intracellular reactive oxygen species (ROS) was evaluated by using the CellROX® Deep Red fluorescent probe (Invitrogen, Termo Fisher Scientific, Madrid, Spain). The trophozoites were treated with the IC_{90} of each molecule for 24 h and exposed to CellROX® Deep Red (5 μM, 30 min) at 26 °C in the dark. Amoebae were observed in an EVOS FL Cell Imaging System AMF4300 (Life Technologies, Madrid, Spain).

2.13. Statistical analysis

All data are expressed as mean ± standard deviation. To highlight the effect of squamins C–F (**1**–**4**) in the ATP production measure assay of *Acanthamoeba* spp. trophozoites, a statistical comparison was performed by a one-way analysis of variance (ANOVA), and a p-value (p) < 0.05 denoted the presence of a statistically significant difference. Statistical analyses were carried out using Sigma Plot 12.0 statistical analysis software (Systat Software Inc, Palo Alto, CA, US).

3. Results

3.1. In vitro activity against Acanthamoeba spp. and cytotoxicity assay of squamins C–F (1–4)

The AcOEt fraction obtained from partition of the methanolic extract of the seeds of *Annona globiflora* was subjected to sequential chromatography in a Lobar LiChroprep-RP18 and a μ-Bondapack C-18 HPLC to afford four cyclic peptides **1**–**4** (Fig. 1). Afterwards, their structures were determined the basis of their spectroscopical and spectrometrical data and identified as squamins C (**1**), D (**2**), E (**3**) and F (**4**) (Sosa-Rueda

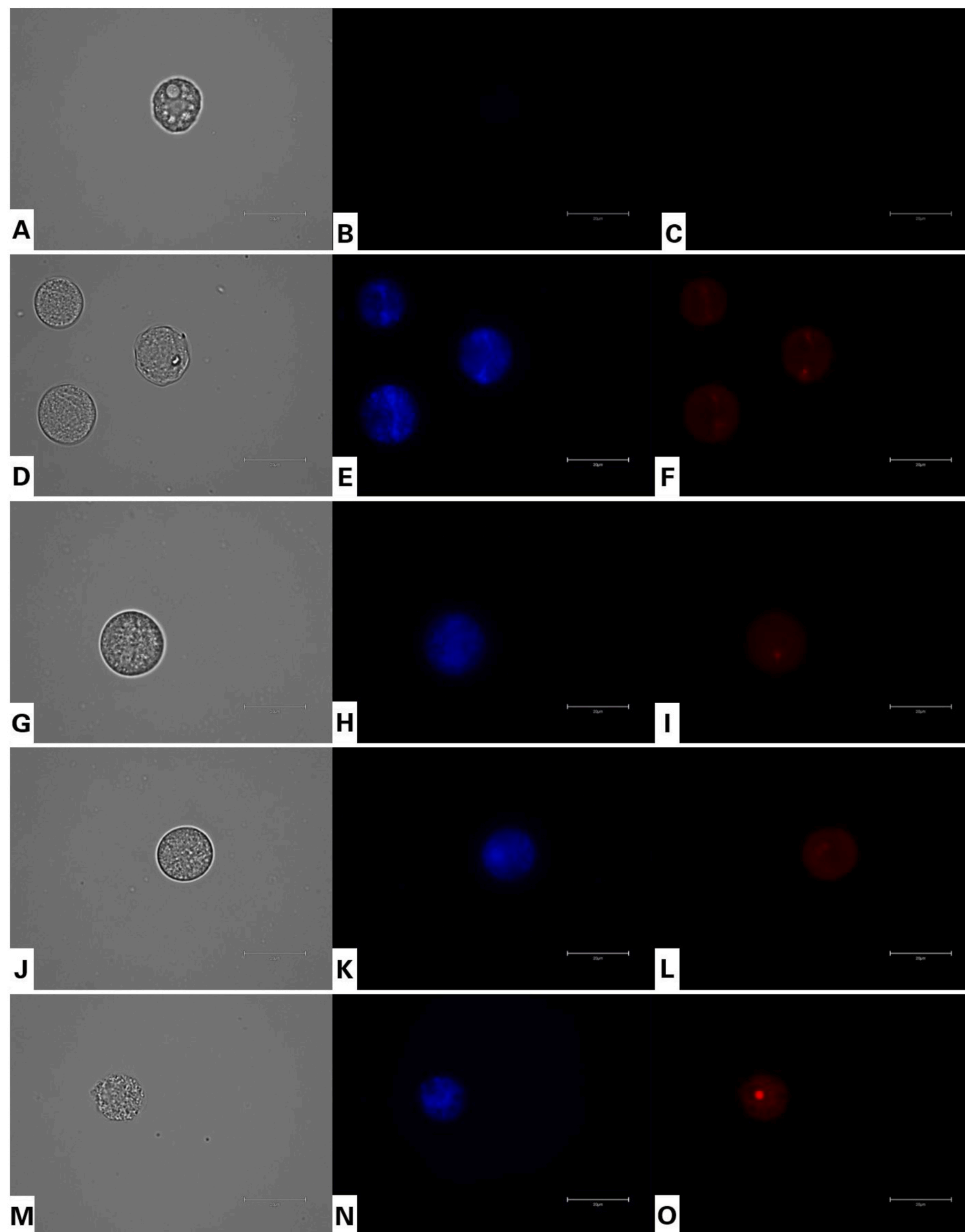

Fig. 6. Images at 100x magnification of *Acanthamoeba castellanii* Neff trophozoites incubated with IC_{90} of squamin C (D, E, F), squamin D (G, H, I), squamin E (J, K, L) and squamin F (M, N, O) on the chromatin condensation. Negative control (A, B, C). All images are based on Live Cell Imaging Microscope EVOS FL Cell Imaging System (Scale Bar 20 μm).

et al., 2021). The activity of compounds **1**–**4** was evaluated against trophozoites of four species of *Acanthamoeba*, including three clinically relevant strains. The *in vitro* amoebicidal activities results are summarized in Table 1.

All the tested peptides were active against the trophozoite stage of the evaluated *Acanthamoeba* strains. Squamin F (**4**) presented the lowest inhibitory concentration 50 (IC_{50}) value in *A. castellanii* Neff at 18.02 ± 3.28 μM. Nevertheless, the most active molecules against the clinical strains used in this study were squamin E (**3**) for *A. polyphaga* (62.19 ± 15.52 μM) and squamin C (**2**) for *A. griffini* and *A. quina* (38.81 ± 7.34 and 24.28 ± 0.64 μM, respectively).

In regard with the *in vitro* cysticidal activity assay (Table 2), squamins C–F (**1**–**4**) only presented activity against the cyst stage of *A. castellanii* Neff and *A. polyphaga* strains. Squamin D (**2**) was the compound that showed the lowest IC_{50} values in both *A. castellanii* and *A. polyphaga* cysts (39.02 ± 6.61 and 72.94 ± 0.53 μM, respectively). On the other hand, *A. griffini* and *A. quina* cysts exhibited high resistance to the tested molecules, revealing IC_{50} values greater than 100 μM.

Nonetheless, it is remarkable that all four peptides showed no cytotoxic effect against murine macrophages cell line J774A.1 (ATCC TIB-67) showing a cytotoxic concentration 50 (CC_{50}) value above 200 μM (Table 1).

Taking all this results into account, squamins C–F (**1**–**4**) were used for further studies focused on the evaluation of the induction of mechanisms of programmed cell death (PCD) in *A. castellanii* Neff trophozoites. All assays were conducted by incubation of cells with the IC_{90} of each molecule (**1**: 43.98 ± 3.21 μM; **2**: 46.45 ± 0.36 μM; **3**: 48.34 ± 6.58 μM; **4**: 45.92 ± 1.31 μM).

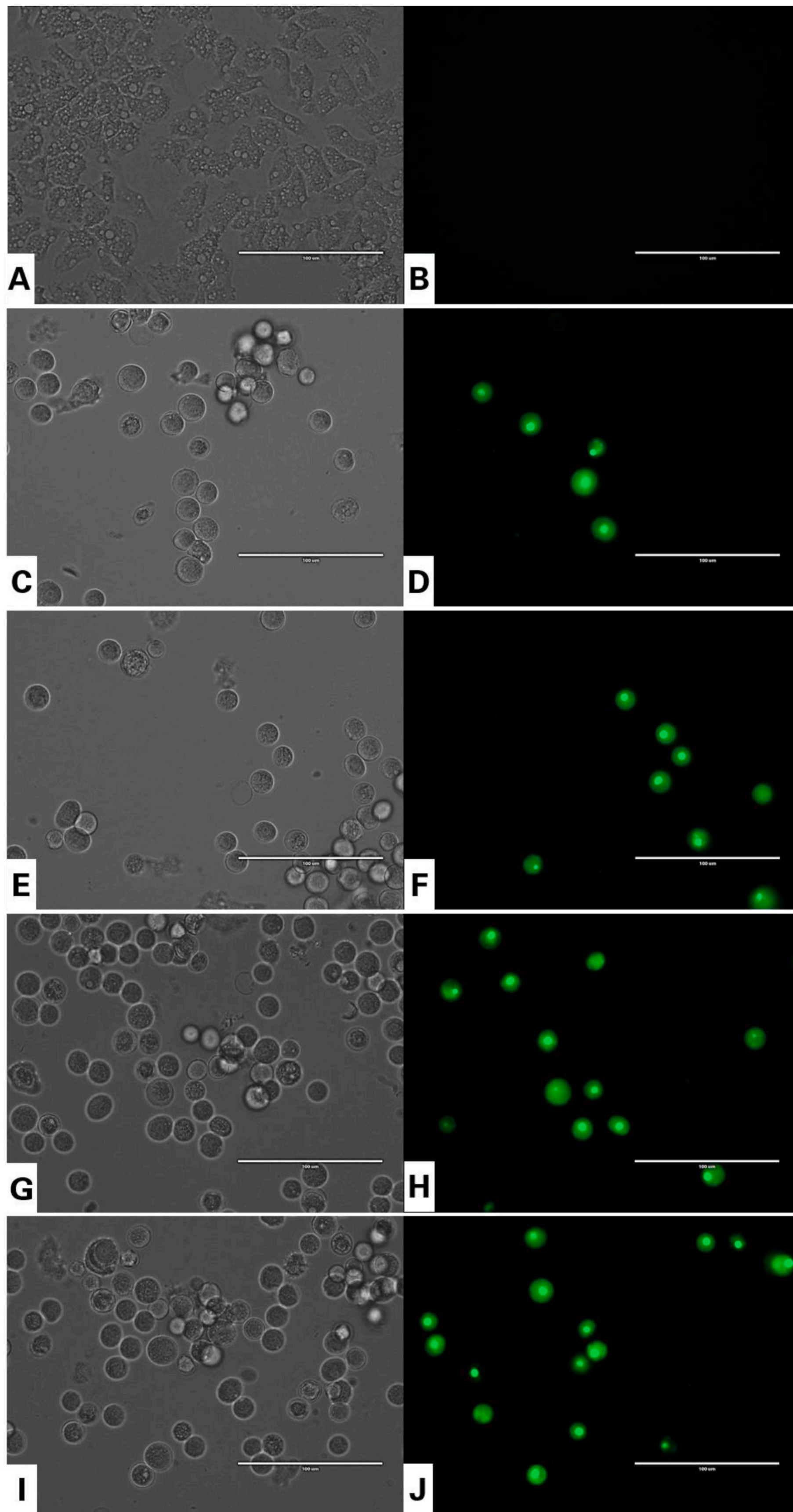

Fig. 7. Effect of IC_{90} of squamin C (C, D), squamin D (E, F), squamin E (G, H) and squamin F (I, J) on the membrane permeability of *Acanthamoeba castellanii* Neff trophozoites compared with the Negative control (A, B) using Sytox Green dye, which stains the nucleic acid of cells with damaged plasma membrane with a green fluorescence. All images (40x) are based on Live Cell Imaging Microscope EVOS FL Cell Imaging System (Scale Bar 100 μm). (For interpretation of the references to colour in this figure legend, the reader is referred to the Web version of this article.)

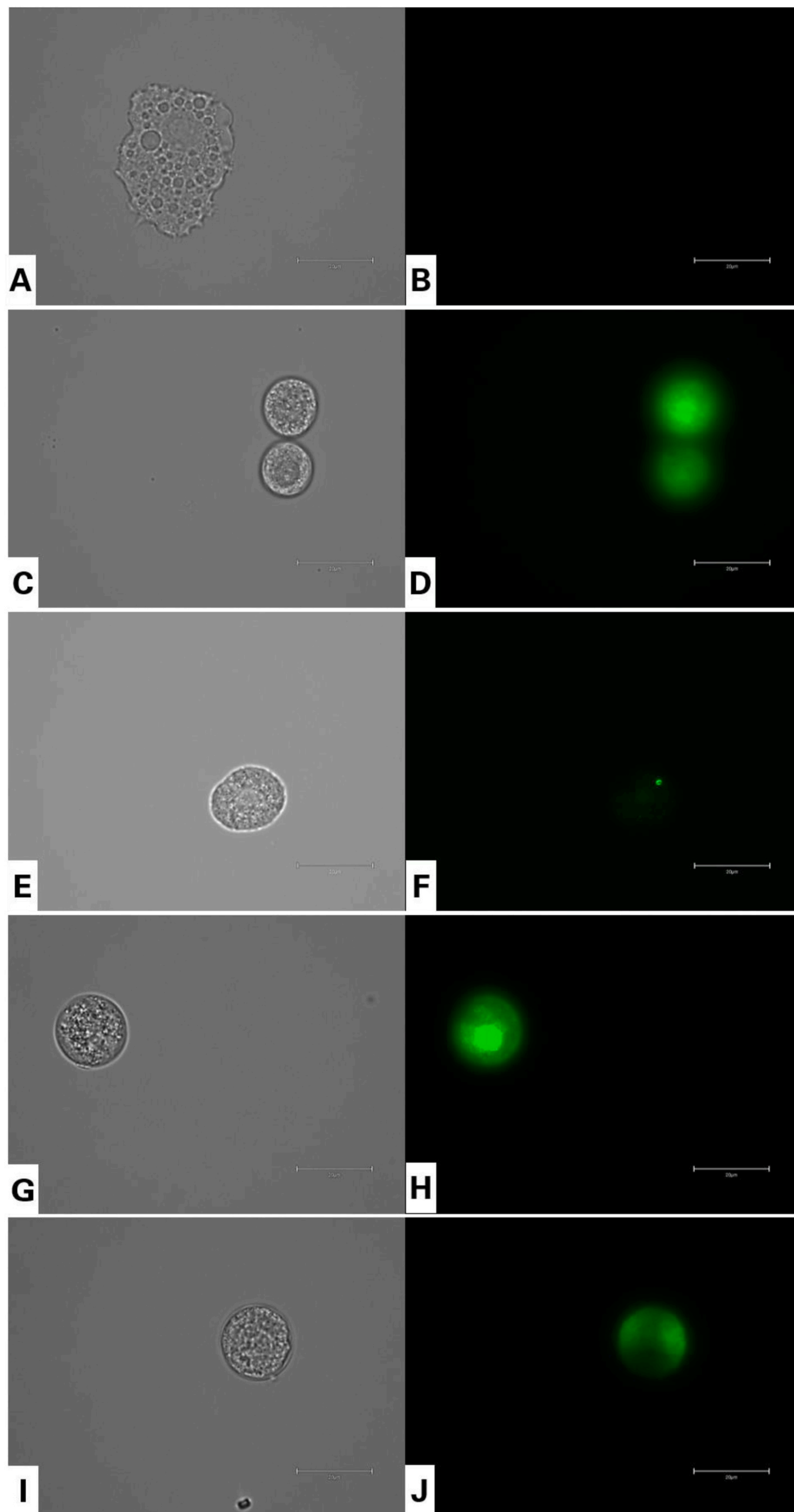

Fig. 8. Sytox Green effect at 100 x magnification. All images (100x) are based on Live Cell Imaging Microscope EVOS FL Cell Imaging System (Scale Bar 20 μm). (For interpretation of the references to colour in this figure legend, the reader is referred to the Web version of this article.)

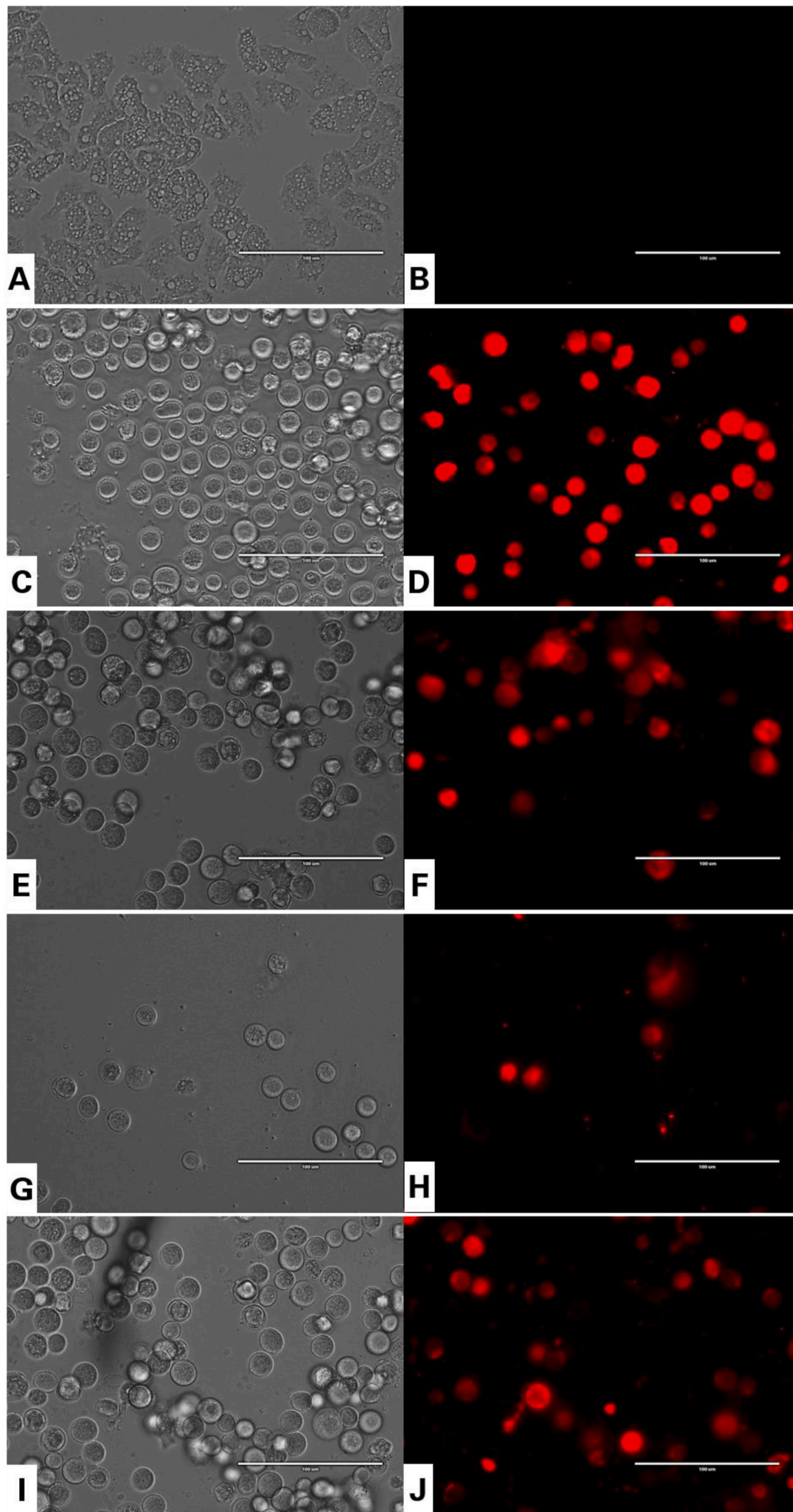

Fig. 9. Reactive Oxygen Species production in *Acanthamoeba castellanii* Neff trophozoites treated with the IC_{90} of squamin C (C, D), squamin D (E, F), squamin E (G, H) and squamin F (I, J), compared with the Negative control (A, B) using CellROX® Deep Red assay kit. All images (40x) are based on Live Cell Imaging Microscope EVOS FL Cell Imaging System (Scale Bar 100 μm). (For interpretation of the references to colour in this figure legend, the reader is referred to the Web version of this article.)

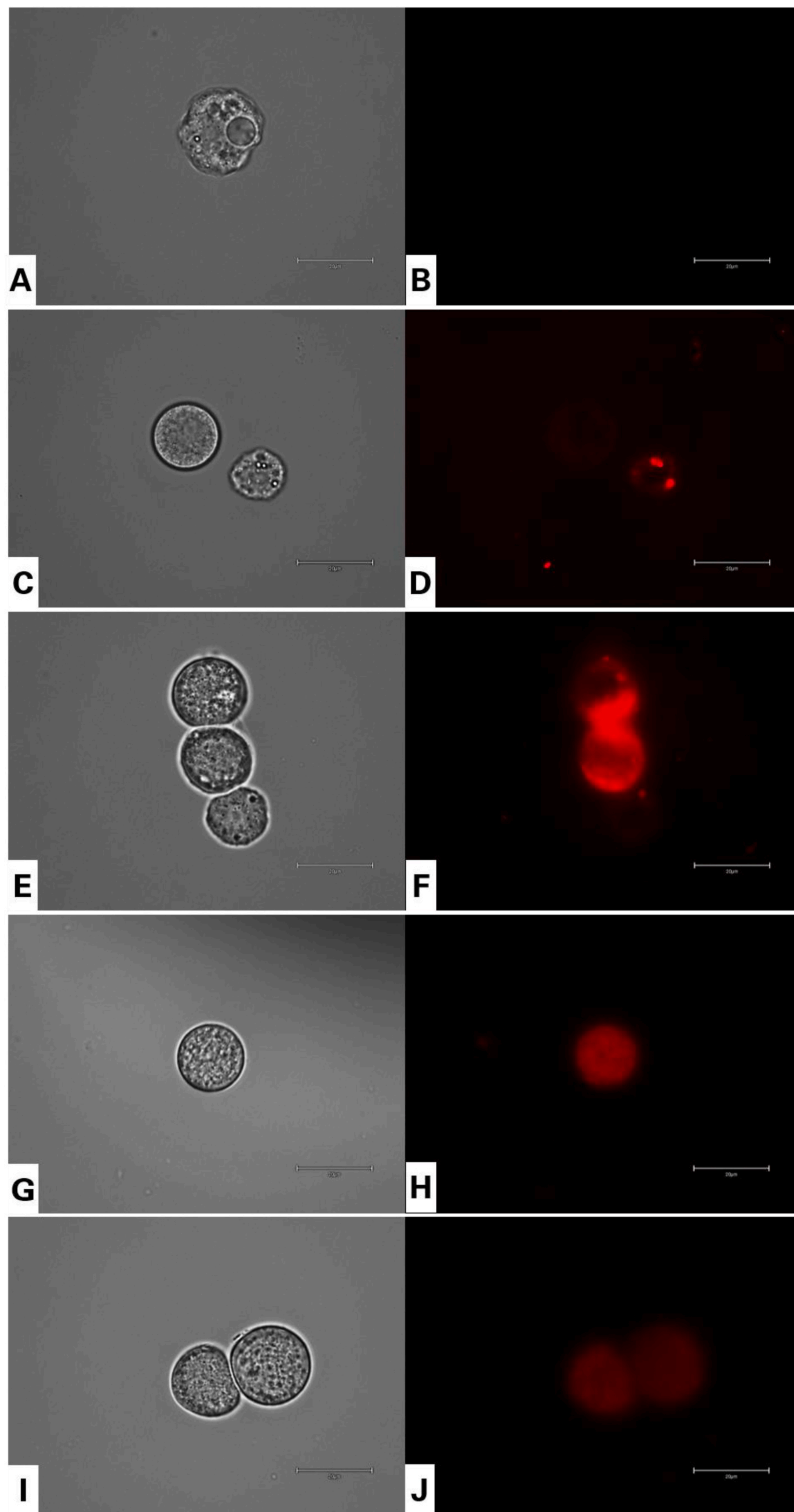

Fig. 10. CellROX® Deep Red fluorescent probe for oxidative stress detection. All images (100x) are based on Live Cell Imaging Microscope EVOS FL Cell Imaging System (Scale Bar 20 μm). (For interpretation of the references to colour in this figure legend, the reader is referred to the Web version of this article.)

3.2. Squamins C–F (1–4) cause mitochondrial malfunction in treated amoebae

Squamins C–F (**1**–**4**) induced mitochondrial damages. As illustrated in Figs. 2 and 3, the four molecules depolarized the mitochondrial membrane potential of *A. castellanii* Neff-treated trophozoites by inhibition of JC-1 agglomeration, showed in the assay as a green fluorescence in its monomeric form (Figs. 2 and 3, right column). In the case of non-treated trophozoites, JC-1 dye accumulates in the mitochondria as aggregates showing a red fluorescence (Figs. 2 and 3, central column). Furthermore, the mitochondrial damage was also checked by measuring the ATP level generated in 24 h. When we incubated the trophozoites with the IC_{90} of compounds **1**–**4**, the amoebae presented a significant inhibition of ATP production compared with the negative control (Fig. 4). The trophozoites treated with squamins E (**3**) showed the highest decrease of ATP level (52.56%) compared with the untreated amoebae. One-way analysis of variance (ANOVA) was carried out to test the statistical differences between means, $p < 0.01$ (**) and $p < 0.001$ (***).

3.3. Evaluated peptides produced chromatin condensation in *A. castellanii* Neff

Once the double staining protocol was performed, all peptides induced chromatin condensation of treated amoebae at a concentration of IC_{90}. The trophozoites treated showed bright-blue stained nuclei at 24 h post incubation with the evaluated molecules (Figs. 5 and 6; E, H, K and N). The propidium iodide (PI) stains amoebae nuclei with a red fluorescence, suggesting a late apoptotic stage (Figs. 5 and 6; F, I, L and O).

Plasma membrane permeability in treated cells As shown in Figs. 7 and 8, trophozoites of *A. castellanii* Neff treated with the IC_{90} of the four cyclic peptides exhibited green fluorescence inside the cells indicating that the plasma membrane permeability in treated cells was slightly damaged after 24 h of incubation. However, in the taken picture we can observe that the cells maintained their integrity.

3.4. Reactive oxygen species (ROS) level increase in treated *A. castellanii* Neff trophozoites

The staining with the CellROX® Deep Red exhibited that all the evaluated molecules increased reactive oxygen species (ROS) levels in *A. castellanii* Neff trophozoites. Treated amoebae with the IC_{90} for 24 h generated higher level of ROS than the negative control demonstrated by the red fluorescence emitted (Figs. 9 and 10).

4. Discussion

Annonaceae family has been extensively studied due to its widespread medicinal properties. The isolated metabolites from this family include a wide range of chemical structures and different biogenetic origins. Among this structural diversity, cyclic peptides possess special relevance. The cytotoxicity, vasorelaxant activity, anti-inflammatory and other properties exhibited by cyclooligopeptides from seeds of *Annona* genus, denote these metabolites as attractive leads for the drug discovery process (Dahiya and Dahiya, 2021). Squamins A and B were the first examples of this structural series. Squamins A and B are configurational isomers which differ in the stereochemistry of the methionine residue. Structural analysis of squamin A indicated that it was a cyclooctapeptide with a proline residue, a modified methionine residue, S-oxo-methionine and the two hydroxy aliphatic and aromatic amino acid L-threonine and L-tyrosine. The absolute stereochemistry was determined by Marfey's reagent and the results confirmed that all residues exhibited S configuration (Chao-Ming et al., 1997). In addition, squamin A was described as the first example of pseudopolymorphism for cyclopeptides pointing out the important role of water molecules in the stabilization of the cyclopeptide network (Jiang et al., 2003). Despite this particular property in squamin A, the biological studies of these peptides have been limited to one single trial. In this study, Yang et al. evaluated the anti-inflammatory properties of squamin A showing low activity as inhibitor on the production of TNFα and IL-6 within LPS-stimulated J774A.1 (Yang et al., 2008).

In the present work we study the activity against amoebae of four congeners of this group of cyclooctapeptides isolated from Mexican specimens of *Annona globiflora*, squamins C–F (**1**–**4**) (Sosa-Rueda et al., 2021). The structural differences are very subtle, differing in the substitution of an isoleucine residue in compounds C and D by a threonine unit in the pair E and F; and additionally, the oxo-methionine configuration R or S, in both pairs (Fig. 1).

The results of antiparasitic assays against *Acanthamoeba* spp. showed that all the peptides showed significant activity in trophozoites stages, especially against *A. castellanii* Neff, exhibiting IC_{50} values of 18.38 and 18.02 μM for squamin D and F, respectively. Among clinical strains, *A. quina* was the most sensitive followed by *A. griffini* and *A. polyphaga* (Table 1). Despite the slight structural changes found in squamins C–F, isoleucine by threonine, and quirality of the oxo-methionine residue, the compounds show significant differences of behaviour against the stages and the strains of the tested parasites. Trophozoites of strain *A. castellanii* Neff are the most sensitive against squamins C–F (**1**–**4**). Data indicate that the substitution of leucine by threonine is not relevant for the biological activity, whereas the R conformers of the S-oxo-methionine residue, squamins D (**2**) and F (**4**), are the most effective. In *A. quina*, the observed effects are similar with respect to the residue interchange, however the *S* S-oxo-methionine isomers are slightly more active than the *R* congeners. On the other hand, the cyclopeptides which contained the isoleucine residue, **1** and **2**, are more active against *A. griffini,* with the least active compound being squamin F (**4**), bearing threonine and *R* configuration at the S-oxo-methionine. *A. polyphaga* is the less sensitive strain showing IC_{50} values ranging from 62.19 to 71.78 μM. Squamins E (**3**) and F (**4**), that contain threonine residues, are the cyclopeptides that showed the lowest values of activity for trophozoites of this species.

Regarding the activity against the cyst stage (Table 2), the cyclopeptides **1**–**4** did not show activity at concentrations below 100 μM against strains *A. griffini* and *A. quina*, whereas *A. castellanii* and *A. polyphaga* were more sensitive upon exposure to compounds. The R isomer that contains isoleucine, squamin D (**2**) was the most active compound against cysts of *A. castellanii* with an IC_{50} of 39.02 μM, whereas its S-isomer (**1**) was the least active with an IC_{50} value of 73.07 μM. All compounds showed a similar IC_{50} value against cysts of *A. polyphaga* in a range around 73 μM.

Squamins C–F (**1**–**4**) revealed low toxicity against the murine macrophages cell line J774A.1 ($CC_{50} > 200$ μM).

The analysis of the mode of action of squamins C–F (**1**–**4**) against *A. castellanii* indicate that these cyclopeptides induced the mechanisms of programmed cell death (PCD). All peptides triggered mitochondrial damages, significant inhibition of ATP production compared to the negative control, chromatin condensation and slight damages in membrane that affects its permeability despite it conserves integrity at the IC_{90} for 24 h. An increase in reactive oxygen species (ROS) was observed in all cases.

5. Conclusions

The cyclooctapeptides identified in *Annona globifolia,* squamins C–F (**1**–**4**), revealed to be an excellent alternative for the design of new drug leads for treatment of amoeba-caused infections, such as *Acanthamoeba* keratitis due to their low toxicity and significant activity against both the trophozoite and cyst stages of *Acanthamoeba* species, particularly *A. castellanii* Neff. Our results highlight that squamins could be candidates in the search for lead therapeutic compounds. In addition, *A. globiflora* is an important source of bioactive molecules, which could promote the sustainable exploitation of this undervalued species.

Declaration of competing interest

The authors declare that there is not conflict of interest with the submission.

Acknowledgements

This study was supported by This study was supported by the Government of the State of Veracruz de Ignacio de la Llave, Veracruz Council for Scientific Research and Technological Development [COVEICyDET, grant number 14 1953/2021],.; PI18/01380 (Fondo Europeo de Desarrollo Regional, FEDER) and RICET (project no. RD16/0027/0001 of the programme of Redes Temáticas de Investigación Cooperativa, FIS), and Project PID2019-109476RB-C21 (BIOALGRI) (Spanish Ministry of Science, Madrid, Spain). ARDM was funded by Agustín de Betancourt Programme, Cabildo de Tenerife, Tenerife 2030, FDCAN, MEDI. RLRE was funded by a grant from Agencia Canaria de Investigación, Innovación y Sociedad de la Información (ACIISI) cofunded by Fondo Social Europeo (FSE) y FEDER, (TESIS2020010117).

References

Anaya-Esparza, L.M., García-Magaña, M.L., Abraham Domínguez-Ávila, J., Yahia, E.M., Salazar-López, N.J., González-Aguilar, G.A., Montalvo-González, E., 2020. Annona: underutilized species as a potential source of bioactive compounds. Food Res. Int. 138, 109775. https://doi.org/10.1016/j.foodres.2020.109775. Pt A.

Baig, A.M., Lalani, S., Khan, N.A., 2017. Apoptosis in *Acanthamoeba castellanii* belonging to the T4 genotype. J. Basic Microbiol. 57 (7), 574–579. https://doi.org/10.1002/jobm.201700025.

Cen-Pacheco, F., Valerio-Alfaro, G., Santos-Luna, D., Fernández, J.J., 2019. Sclerin, a New Cytotoxic Cyclononapeptide from Annona Scleroderma. Molecules, vol. 24, p. 554. https://doi.org/10.3390/molecules24030554.

Chao-Ming, L., Ning-Hua, T., Qing, M., Hui-Lan, Z., Xiao-Jiang, H., Yu, W., Jun, Z., 1997. Cyclopeptide from the seeds of *Annona squamosa*. Phytochemistry 45 (3), 521–523. https://doi.org/10.1016/S0031-9422(96)00829-1.

Chegeni, T.N., Fakhar, M., Ghaffarifar, F., Saberi, R., 2020. Medicinal plants with anti-*acanthamoeba* activity: a systematic review. Infect. Disord. - Drug Targets 20 (5), 620–650. https://doi.org/10.2174/1871526519666190716095849.

Dahiya, R., Dahiya, S., 2021. Natural bioeffective cyclooligopeptides from plant seeds of *Annona* genus. Eur. J. Med. Chem. 214, 113221. https://doi.org/10.1016/j.ejmech.2021.113221.

Escobedo-López, D., Campos-Rojas, E., Rodríguez-Núñez, J.R., Alia-Tejacal, I., Núñez-Colin, C.A., 2019. Priority areas to collect germplasm of *Annona* (annonaceae) in Mexico based on diversity and species richness indices. Genet. Resour. Crop Evol. 66, 401–413. https://doi.org/10.1007/s10722-018-0718-2.

González-Robles, A., Salazar-Villatoro, L., Omaña-Molina, M., Reyes-Batlle, M., Martín-Navarro, C.M., Lorenzo-Morales, J., 2014. Morphological features and *in vitro* cytopathic effect of *Acanthamoeba griffini* trophozoites isolated from a clinical case. Journal of parasitology research 2014, 256310. https://doi.org/10.1155/2014/256310.

Jiang, R.-W., Lu, Y., Min, Z.-D., Zheng, Q.-T., 2003. Molecular structure and pseudopolymorphism of squamtin A from *Annona squamosa*. J. Mol. Struct. 655 (1), 157–162. https://doi.org/10.1016/S0022-2860(03)00227-8.

Kot, K., Łanocha-Arendarczyk, N.A., Kosik-Bogacka, D.I., 2018. Amoebas from the genus *Acanthamoeba* and their pathogenic properties. Annals of parasitology 64 (4), 299–308. https://doi.org/10.17420/ap6404.164.

Kupchan, S.M., Tsou, G., Sigel, C.W., 1973. Datiscacin, a novel cytotoxic cucurbitacin 20-acetate from *Datisca glomerate*. J. Org. Chem. 38, 1420–1421. https://doi.org/10.1021/jo00947a041.

Leite, D., de, F.A., Nonato, C., Camilo, C.J., de Carvalho, N., da Nobrega, M., Pereira, R. C., da Costa, J., 2020. Annona genus: traditional uses, phytochemistry and biological activities. Curr. Pharmaceut. Des. 26 (33), 4056–4091. https://doi.org/10.2174/1381612826666200325094422.

Lorenzo-Morales, J., Khan, N.A., Walochnik, J., 2015. An update on *Acanthamoeba* keratitis: diagnosis, pathogenesis and treatment. Parasite 22 (10). https://doi.org/10.1051/parasite/2015010.

Martín-Navarro, C.M., Lorenzo-Morales, J., Cabrera-Serra, M.G., Rancel, F., Coronado-Álvarez, N.M., Piñero, J.E., Valladares, B., 2008. The potential pathogenicity of chlorhexidine-sensitive *Acanthamoeba* strains isolated from contact lens cases from asymptomatic individuals in Tenerife, Canary Islands, Spain. J. Med. Microbiol. 57 (Pt 11), 1399–1404. https://doi.org/10.1099/jmm.0.2008/003459-0.

Martín-Navarro, C.M., López-Arencibia, A., Sifaoui, I., Reyes-Batlle, M., Valladares, B., Martínez-Carretero, E., Piñero, J.E., Maciver, S.K., Lorenzo-Morales, J., 2015. Statins and voriconazole induce programmed cell death in *Acanthamoeba castellanii*. Antimicrob. Agents Chemother. 59 (5), 2817–2824. https://doi.org/10.1128/AAC.00066-15.

Ohashi, M., Amoa-Bosompem, M., Kwofie, K.D., Agyapong, J., Adegle, R., Sakyiamah, M. M., Ayertey, F., Owusu, K.B., Tuffour, I., Atchoglo, P., Tung, N.H., Uto, T., Aboagye, F., Appiah, A.A., Appiah-Opong, R., Nyarko, A.K., Anyan, W.K., Ayi, I., Boakye, D.A., Koram, K.A., Edoh, D., Yamaoka, S., Shoyama, Y., Ohta, N., 2018. *In vitro* antiprotozoan activity and mechanisms of action of selected Ghanaian medicinal plants against *Trypanosoma, Leishmania*, and *Plasmodium* parasites. Phytother Res.: PTR 32 (8), 1617–1630. https://doi.org/10.1002/ptr.6093.

Quílez, A.M., Fernández-Arche, M.A., García-Giménez, M.D., De la Puerta, R., 2018. Potential therapeutic applications of the genus *Annona*: local and traditional uses and pharmacology. J. Ethnopharmacol. 225, 244–270. https://doi.org/10.1016/j.jep.2018.06.014.

Rodríguez-Expósito, R.L., Nocchi, N., Reyes-Batlle, M., Sifaoui, I., Suárez-Gómez, B., Díaz-Marrero, A.R., Souto, M.L., Piñero, J.E., Fernández, J.J., Lorenzo-Morales, J., 2021. Antiamoebic effects of sesquiterpene lactones isolated from the zoanthid. Palythoa aff. clavata. Bioorganic chemistry 108, 104682. https://doi.org/10.1016/j.bioorg.2021.104682.

Rodríguez-Martín, J., Rocha-Cabrera, P., Reyes-Batlle, M., López-Arencibia, A., Sifaoui, I., Rizo-Liendo, A., Bethencourt-Estrella, C.J., Piñero, J.E., Lorenzo-Morales, J., 2018. Presence of *Acanthamoeba* in the ocular surface in a Spanish population of contact lens wearers. Acta Parasitol. 63 (2), 393–396. https://doi.org/10.1515/ap-2018-0045.

Sarabia, F., Chammaa, S., Ruiz, A.S., Ortiz, L.M., Herrera, F.J., 2004. Chemistry and biology of cyclic depsipeptides of medicinal and biological interest. Curr. Med. Chem. 11 (10), 1309–1332. https://doi.org/10.2174/0929867043365224.

Siddiqui, R., Khan, N.A., 2012. Biology and pathogenesis of. Acanthamoeba. Parasites & vectors 5 (6). https://doi.org/10.1186/1756-3305-5-6K.

Sifaoui, I., Reyes-Batlle, M., López-Arencibia, A., Chiboub, O., Rodríguez-Martín, J., Rocha-Cabrera, P., Valladares, B., Piñero, J.E., Lorenzo-Morales, J., 2018. Toxic effects of selected proprietary dry eye drops on *Acanthamoeba*. *Scientific reports, 8*(1) 8520. https://doi.org/10.1038/s41598-018-26914-3.

Sifaoui, I., Rodríguez-Talavera, I., Reyes-Batlle, M., Rodríguez-Expósito, R.L., Rocha-Cabrera, P., Piñero, J.E., Lorenzo-Morales, J., 2020. *In vitro* evaluation of commercial foam Belcils® on *Acanthamoeba* spp. International journal for parasitology. Drugs and drug resistance 14, 136–143. https://doi.org/10.1016/j.ijpddr.2020.10.002.

Sosa-Rueda, J., Domínguez-Meléndez, V., Ortiz-Celiseo, A., López-Fentanes, F., Cuadrado, C., Fernández, J.J., Hernández-Daranas, A., Cen-Pacheco, F., 2021. Squamins C-F, four cyclopepetides from the seeds of. Annona globiflora. Phytochemistry. https://doi.org/10.1016/j.phytochem.2021.112839 (in press).

Tan, N.H., Zhou, J., 2006. Plant cyclopeptides. Chem. Rev. 106 (3), 840–895. https://doi.org/10.1021/cr040699h.

Wang, X., Lin, M., Xu, D., Lai, D., Zhou, L., 2017. Structural diversity and biological activities of fungal cyclic peptides, excluding cyclodipeptides. Molecules *22*, 2069. https://doi.org/10.3390/molecules22122069, 12.

Wink, M., 2012. Medicinal plants: a source of anti-parasitic secondary metabolites. Molecules 17 (11), 12771–12791. https://doi.org/10.3390/molecules171112771.

Yang, Y.L., Hua, K.F., Chuang, P.H., Wu, S.H., Wu, K.Y., Chang, F.R., Wu, Y.C., 2008. New cyclic peptides from the seeds of *Annona squamosa* L. and their anti-inflammatory activities. J. Agric. Food Chem. 56 (2), 386–392. https://doi.org/10.1021/jf072594w.